IEEE Access
Multidisciplinary | Rapid Review | Open Access Journal

Received August 21, 2018, accepted September 14, 2018, date of publication October 1, 2018, date of current version October 25, 2018.

Digital Object Identifier 10.1109/ACCESS.2018.2872748

Two-Layer Carrier Index Modulation Scheme Based on Differential Chaos Shift Keying

WENHAO DAI[1], HUA YANG[1], (Member, IEEE), YURONG SONG[2], AND GUOPING JIANG[2], (Senior Member, IEEE)

[1]College of Electronic and Optical Engineering, Nanjing University of Posts and Telecommunications, Nanjing 210023, China
[2]College of Automation, Nanjing University of Posts and Telecommunications, Nanjing 210023, China

Corresponding author: Hua Yang (yangh@njupt.edu.cn)

This work was supported in part by the National Natural Science Foundation of China under Grant 61401226, Grant 61373136, Grant 61672298, and Grant 61374180, in part by the Jiangsu Government Scholarship for Oversea Studies, and in part by the University Science Research Project of Jiangsu Province under Grant 18KJB510033 and Grant 16KJB510045.

ABSTRACT In this paper, a novel carrier index differential chaos shift keying (DCSK) modulation system is proposed for increased energy and spectral efficiencies. The new system splits all data bits into two groups, which are carried by the chaotic signals and their Hilbert transforms, respectively. For each group, one active subcarrier is selected from all candidate subcarriers according to the index bits, and the signal transmitted via the active subcarrier carries one modulated bit through DCSK modulation. By correlating with the exact or the Hilbert filtered chaotic reference signals, the two data groups can be demodulated separately. In each group, the index bits are determined by the maximum energy comparator, while the threshold verdict helps to estimate the modulated bit. Analytical bit error rate expressions over additive white Gaussian noise and multipath Rayleigh fading channels are derived. Simulations and comparisons are also performed to verify the advantages of this new proposed design.

INDEX TERMS Carrier index modulation, chaos, energy efficiency, Hilbert transform, spectral efficiency.

I. INTRODUCTION

Since chaotic signals are easy to generate and offer good characteristics, including wide spectrum, good auto- correlation and high sensitivity to initial value, these signals have attracted more and more attentions in communications [1]. As a kind of spread spectrum communication systems, chaos-based communication systems use wideband non-periodic chaotic signals as carriers, and thus show superiorities in anti-jamming capability, low probability of interception, etc. Among all these systems, differential chaos shift keying (DCSK) with low complexity and good anti-multipath fading capability appears to be more popular [2], [3].

However, DCSK system suffers from two major drawbacks. On one hand, half of bit energy and half of duration are spent on transmitting the reference signal, resulting in low data rate, reduced energy efficiency and degraded bit error rate (BER) performance. On the other hand, DCSK transmitter and receiver require radio frequency (RF) delay lines, which are not easy to implement in ultra-wide band (UWB) communications. For high data rate, a high-efficiency DCSK (HE-DCSK) system is proposed in [4], where reference signal in previous bit duration is reused to carry one more data bit in current data-bearing slot. With the same purpose, a short reference DCSK (SR-DCSK) system is proposed in [5], in which reference signals are shortened so that they occupy less time. Later, SR-DCSK system is optimized in [6] for better performance. Unfortunately, these systems fail to solve the delay line problem in DCSK. For delay line removal from receivers, a code-shifted DCSK (CS-DCSK) system is proposed in [7], which employs orthogonal Walsh codes to bear the data and reference signals, respectively. In [8], a generalized CS-DCSK system (GCS-DCSK) is studied for bit rate increase. To avoid delay lines in both transmitters and receivers, a multi-carrier DCSK (MC-DCSK) system is designed in [9]. Rather than time delay, MC-DCSK separates the reference and data-bearing signals in frequency domain and transmits multiple data bits in a parallel way over different subcarriers, which helps to improve the data rate and energy efficiency effectively.

For higher spectral efficiency, quadrature chaotic shift keying (QCSK) system is presented in [10]. Later, it has been extended to multiresolution M-ary DCSK

(MR M-ary-DCSK) system in [11] so as to make a tradeoff between transmission rate and quality of service. Based on square constellations, a novel M-ary DCSK system framework is proposed in [12], which further increases the spectral efficiency with lower energy consumption. To maximize the spectral efficiency, adaptive transmission schemes are designed for MR M-ary-DCSK and square-constellation-based M-ary DCSK systems in [13] and [14], respectively. By modifying the distance between the two constellation points according to the signal-to-noise ratio information, these two systems can satisfy different BER requirements for different bits within a symbol. Besides, other strategies, i.e., automatic repeat request/cooperative automatic repeat request (ARQ/CAQR) techniques in [15], multiple-input multiple-output (MIMO) and relay cooperative diversity techniques in [16], etc., have also been combined with DCSK for improvement in spectral efficiency.

As a competitive technique for 5G wireless network, index modulation has attracted tremendous interest over the past few years [17]. By altering the on/off status of the transmission entities such as spreading codes, carriers, antennas and so on, index modulation can not only simplify the system structure but also offer benefits in term of spectral and energy efficiencies. In [18] and [19], code index modulations for direct sequence spread spectrum (DS -SS) communications are proposed, in which indices of spreading codes are used to carry more information. In [20], code index modulation is applied in GCS-DCSK system for higher spectral efficiency. In [21], code index modulation is combined with SR-DCSK system, and corresponding noise reduction and power allocation strategies are, respectively, studied for better performance. Based on multilevel code shifted DCSK scheme in [22], a new multilevel code index modulation system is proposed in [23], where Walsh code indices are utilized to carry multiple information bits. The initial condition-index chaos shift keying (ICI-CSK) system is proposed in [24], which exploits initial conditions to generate different chaotic sequences to convey extra bits. In [25], chaotic sequences and their Hilbert transforms are combined with Walsh codes so that more spreading sequences can be constructed for code index modulation. In permutation index DCSK (PI-DCSK) system in [26], one of predefined reference sequence permutations is selected according to the index bits, while a single modulated bit is spread by the selected sequence. Based on PI-DCSK, commutation code index DCSK (CCI-DCSK) system is proposed in [27] for a simultaneous transmission of the reference and data signals.

Besides, carrier index modulation has been introduced into orthogonal frequency division multiplexing (OFDM) systems, in which data bits are carried by both M-ary signal constellations and the indices of active subcarriers [28]. For lower complexity, frequency index modulation (FIM) is proposed in [29] and then improved in [30] by combing code index modulation. Recently, the idea of carrier index modulation has been applied in MC-DCSK system, and two types of carrier index DCSK (CI-DCSK) modulations have been proposed in [31]. These two systems use different parameter settings and index selectors to implement carrier index modulation. Compared to MC-DCSK, CI-DCSK saves transmission energy and improves BER performance.

To better recycle the subcarrier resources in CI-DCSK, a two-layer carrier index differential chaos shift keying (2CI-DCSK) modulation is proposed in this paper. In this new system, indices of all available subcarriers are used twice so that two layers of carrier index modulations could be implemented by sharing the same available subcarriers. Modulations in these two layers are independent. Data in each layer is conveyed not only by the indices of subcarriers but also by the polarities of the message bearers. To reduce inter-layer interferences, orthogonal chaotic message bearers (i.e., chaotic signals and their Hilbert transforms) are utilized in two layers. Compared to CI-DCSK, the proposed system obtains higher spectral and energy efficiencies due to better exploration in subcarrier resources.

The rest of this paper is organized as follows: In the coming section, the basic scheme of DCSK is first briefly reviewed, and the system model of the proposed 2CI-DCSK scheme is then presented. In section III and section IV, efficiencies, complexities and BER performance of the proposed system are analyzed, respectively. Simulation results and related discussions are given in section V. Finally, the paper is concluded in section VI.

II. SYSTEM MODEL

A. BRIEF REVIEW OF DCSK

In DCSK, one bit duration is divided into two slots. The first slot is used to transmit the reference signal, while the second one is used to transmit the data-bearing signal with the same length as the reference signal. If the data bit is "+1", the data-bearing signal is exactly the same as the reference signal; if the data bit is "−1", a negative copy of the reference signal is employed as the data-bearing signal. During the i^{th} bit duration, the output signal of the DCSK transmitter can be given by:

$$s_{i,k} = \begin{cases} x_{i,k}, & 0 < k \leq \beta \\ b_i x_{i,k-\beta}, & \beta < k \leq 2\beta \end{cases} \tag{1}$$

where $x_{i,k}$ is the k^{th} sample of chaotic reference signal in the i^{th} bit duration, and b_i is the data bit transmitted in current bit duration. β is the length of the chaotic reference.

At the receiver, the received reference signal is correlated with its delayed version and then summed over half bit duration. Finally, the data bits can be demodulated according to the signs of the correlator outputs.

B. SYSTEM MODEL OF 2CI-DCSK

In CI-DCSK [31], the total number of available subcarriers is n, in which m subcarriers will be activated according to p index bits. Besides, signal transmitted via each active subcarrier also carries one modulated bit through DCSK modulation. For higher bit rate and better spectral efficiency,

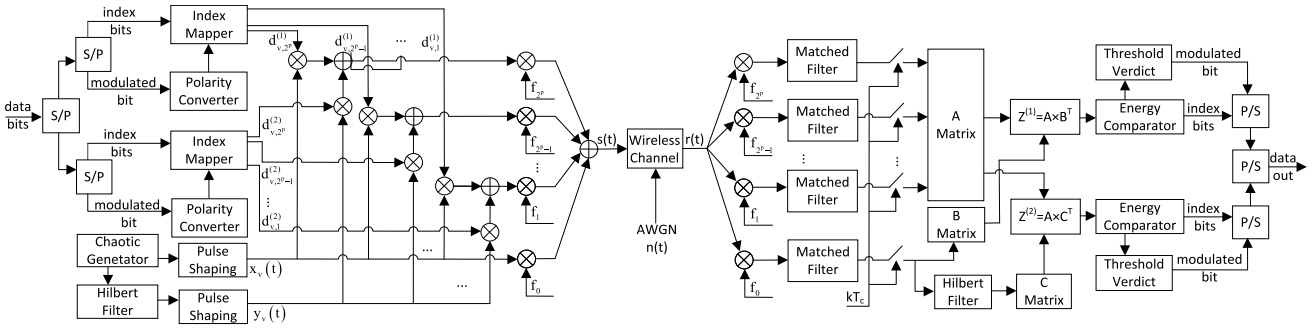

FIGURE 1. Block diagram of 2CI-DCSK system.

2CI-DCSK system reuses all available subcarriers to achieve two layers of index modulations. To avoid the detection of an invalid subcarrier activation pattern, two settings, i.e., $m = 1$, $n = 2^p$ and $m = n - 1$, $n = 2^p$, are employed in [31], both of which can be applied in 2CI-DCSK. In this paper, the first setting, i.e., $m = 1, n = 2^p$, is adopted so that the catastrophic results caused by invalid detection can be avoided.

The transmitter and receiver of the proposed system are given in Fig.1. This new system splits all data bits into two parallel groups, which are transmitted simultaneously via two layers of CI-DCSK modulations. Modulations in these layers are similar and share not only the same reference but also the same subcarriers. But they are actually independent and use orthogonal message bearers, i.e., chaotic signals and their Hilbert transforms.

During the v^{th} symbol period, the chaotic sequence outputted by the chaotic generator is first fed into the upper pulse shaping filter in Fig.1, and the generated chaotic signal $x_v(t)$ will be sent as current reference signal over the reference subcarrier with center frequency of f_0.

$$x_v(t) = \sum_{k=1}^{\beta} x_{v,k} h(t - kT_c) \tag{2}$$

where T_c is the chip time, and $h(t)$ is the impulse response of the pulse shaping filter with a normalized energy.

Based on the Hilbert transform of $x_{v,k}$, the second message bear $y_v(t)$ that is orthogonal to $x_v(t)$ is generated by the lower pulse shaping filter in Fig.1:

$$y_v(t) = \sum_{k=1}^{\beta} \tilde{x}_{v,k} h(t - kT_c) \tag{3}$$

For two-layer transmissions, $2p+2$ serial bits are paralleled and equally divided into two groups $S_v^{(1)}$ and $S_v^{(2)}$. In each group, the first p bits are index bits for carrier index modulation, and the remaining one is the modulated bit for DCSK modulation. Here, $S_v^{(1)}$ transmitted through the first layer is carried by $x_v(t)$, while $S_v^{(2)}$ transmitted through the second layer is carried by $y_v(t)$.

In Fig.1, two identical index mappers are utilized to perform carrier index modulations and DCSK modulations in two layers. In order to activate one subcarrier out of 2^p available subcarriers, the index mapper first maps the input p index bits into 2^p coefficients for 2^p available subcarriers. Among these coefficients, only one is non-zero, while the other ones are equal to zero. The non-zero coefficient is positioned according to the input p index bits, but its value (i.e., either -1 or $+1$) is determined by the input modulated bit after polarity converting. For instance, the output of the upper index mapper are $d_{v,1}^{(1)}, \ldots, d_{v,i}^{(1)}, \ldots, d_{v,2^p}^{(1)}$, in which $d_{v,i}^{(1)}$ denotes the coefficient for the i^{th} subcarrier in the first layer in the v^{th} symbol duration. If the i^{th} subcarrier is active in the first layer, $d_{v,i}^{(1)}$ is equal to the polarized modulated bit $b_v^{(1)}$. Otherwise, $d_{v,i}^{(1)}$ equals to zero. In Table 1, a simple mapping rule for $p = 2$ is given.

TABLE 1. Mapping rule for index mapper (p=2).

Modulated bit	Polarized modulated bit	Index bits	Index of active subcarrier	Coefficients
0	-1	00	1	-1 0 0 0
0	-1	01	2	0 -1 0 0
0	-1	10	3	0 0 -1 0
0	-1	11	4	0 0 0 -1
1	+1	00	1	+1 0 0 0
1	+1	01	2	0 +1 0 0
1	+1	10	3	0 0 +1 0
1	+1	11	4	0 0 0 +1

Next, message bear in each layer will be weighted by these coefficients and then modulated on the sinusoidal subcarriers with center frequencies of $f_1, \ldots, f_2^p$, respectively. Finally, these modulated signals are summed and transmitted by the 2CI-DCSK transmitter. The transmitted signal in the v^{th} symbol duration is then presented by:

$$s(t) = \sum_{i=1}^{2^p} \left(d_{v,i}^{(1)} x_v(t) + d_{v,i}^{(2)} y_v(t) \right) \cos(2\pi f_i t + \varphi_i) + x_v(t) \cos(2\pi f_0 t + \varphi_0) \tag{4}$$

where φ_i and f_i represent the phase angle and the center frequency of the i^{th} subcarrier, respectively.

At the receiver side, the received signal is first multiplied by $2^p + 1$ corresponding synchronized sinusoidal subcarriers.

After being filtered by matched filters, 2^p+1 signals extracted from all subcarriers are sampled at every kT_c instant. The recovered discrete reference signal output by the bottom sampler in Fig.1 is stored in matrix $\boldsymbol{B}_{1\times\beta}$ and its Hilbert transform is stored in matrix $\boldsymbol{C}_{1\times\beta}$. In addition, the outputs of the upper 2^p samplers in Fig.1 are stored in matrix $\boldsymbol{A}^p_{2\times\beta}$, which are the discrete data-bearing signals retrieved from 2^p available subcarriers.

Then, two correlation matrices $\boldsymbol{Z}_v^{(1)}$ and $\boldsymbol{Z}_v^{(2)}$ are computed as:

$$\boldsymbol{Z}_v^{(1)} = \boldsymbol{A} \times \boldsymbol{B}^T = \begin{bmatrix} Z_{v,1}^{(1)} \\ \vdots \\ Z_{v,2^p}^{(1)} \end{bmatrix} \tag{5}$$

$$\boldsymbol{Z}_v^{(2)} = \boldsymbol{A} \times \boldsymbol{C}^T = \begin{bmatrix} Z_{v,1}^{(2)} \\ \vdots \\ Z_{v,2^p}^{(2)} \end{bmatrix} \tag{6}$$

To recover the index bits in two layers, $\boldsymbol{Z}_v^{(1)}$ and $\boldsymbol{Z}_v^{(2)}$ are fed into two parallel energy comparators, respectively. In each energy comparator, the index bits are estimated in the following three steps: 1. Change all elements in the input matrix into their absolute values. 2. By finding the element with maximum absolute value, the index of the active subcarrier can be estimated as:

$$\hat{c}_v^{(1)} = \arg \max_{i=1,\ldots,2^p} (|z_{v,i}^{(1)}|) \tag{7}$$

$$\hat{c}_v^{(2)} = \arg \max_{i=1,\ldots,2^p} (|z_{v,i}^{(2)}|) \tag{8}$$

Here, $\hat{c}_v^{(1)}$ and $\hat{c}_v^{(2)}$ are, respectively, the estimated indices of active subcarriers in the first and second layers in the v^{th} symbol duration. 3. Recover the index bits according to the reversed version of the mapping rule shown in Table 1.

Later, the modulated bits in two layers are estimated in a parallel way by the following two threshold verdicts based on the following rules:

$$\hat{a}_v^{(1)} = \begin{cases} 0, & if\ sign(z_{v,\hat{c}_v^{(1)}}^{(1)}) = -1 \\ 1, & if\ sign(z_{v,\hat{c}_v^{(1)}}^{(1)}) = +1 \end{cases} \tag{9}$$

$$\hat{a}_v^{(2)} = \begin{cases} 0, & if\ sign(z_{v,\hat{c}_v^{(2)}}^{(2)}) = -1 \\ 1, & if\ sign(z_{v,\hat{c}_v^{(2)}}^{(2)}) = +1 \end{cases} \tag{10}$$

In which, $\hat{a}_v^{(1)}$ and $\hat{a}_v^{(2)}$ represent the recovered modulated bits in the first and second layers in the v^{th} symbol duration, respectively.

III. EFFICIENCY AND COMPLEXITY ANALYSIS

In this section, the energy and spectral efficiencies of the proposed system are first analyzed. Then, the complexities of the proposed system are discussed and compared to those of CIM-DCSK system in [21] and CI-DCSK system in [31]. Here, all results are obtained under the assumption that the number of transmitted bits per symbol is $2p+2$ and the length of chaotic reference sequence is β.

TABLE 2. DBR comparison.

Modulation	DBR
MC-DCSK	$(2p+2)/(2p+3)$
PI-DCSK	$p+1$
CCI-DCSK	$p+1$
CIM-DCSK	$(2p+2)\cdot 2^{2p+1}/(2^{2p+1}+1)$
CI-DCSK	$p+1$
2CI-DCSK	$(4p+4)/3$

A. ENERGY EFFICIENCY

The symbol energy of the transmitted signal in 2CI-DCSK can be computed as:

$$E_s = E_{data} + E_{ref} = E_{data1} + E_{data2} + E_{ref} \tag{11}$$

where E_{data} denotes the data energy per symbol and E_{ref} is the reference energy per symbol. E_{data1} and E_{data2} are the data energies per symbol in the first and the second layers, respectively.

Considering that the energies of signals in (2) and (3) are identical, by neglecting the loss of generality, we calculate the data and reference energies as:

$$E_{data1} = E_{data2} = E_{ref} = \frac{1}{2}\sum_{k=1}^{\beta} x_{v,k}^2 \tag{12}$$

As $2p+2$ bits are transmitted in one symbol duration in 2CI-DCSK, the bit energy can be presented as:

$$E_b = \frac{E_s}{2p+2} = \frac{3}{4p+4}\sum_{k=1}^{\beta} x_{v,k}^2 \tag{13}$$

According to the definition of Data-energy to Bit-energy Ratio (DBR) given in [9] and [26], DBR of 2CI-DCSK system can be calculated as:

$$DBR_{2CI-DCSK} = \frac{E_{data}}{E_b} = \frac{4p+4}{3} \tag{14}$$

In Table 2, the DBRs of different chaotic modulations are compared. As shown in this table, MC-DCSK performs the worst in energy efficiency among these systems. This is due to the fact that all systems employ index modulation to carry extra data bits except MC-DCSK. Although the energy efficiency of 2CI-DCSK is slightly lower than that of CIM-DCSK, it has been noticeably improved in comparison with PI-DCSK, CCI-DCSK and CI-DCSK systems. This is due to the fact that two groups of data bits sent in two layers in 2CI-DCSK share one reference, thus reducing the proportion of the reference energy to the total emission energy.

B. SPECTRAL EFFICIENCY

As defined in [32], the spectral efficiency can be denoted as the ratio of bit rate to total bandwidth. With assumption that the bandwidth for each subcarrier is identical and denoted as B, the spectral efficiency of 2CI-DCSK is computed as

$$\eta_{2CI-DCSK} = \frac{bit\ rate}{total\ bandwidth} = \frac{\frac{2p+2}{\beta T_c}}{(2^p+1)B} = \frac{2p+2}{(2^p+1)B\beta T_c} \tag{15}$$

Table 3 shows the spectral efficiencies of various chaotic modulation systems. With the help of code index modulation, PI-DCSK and CCI-DCSK are superior to MC-DCSK in spectral efficiency. Although CIM-DCSK also utilizes code index modulation, it spends much more time on transmitting data-bearing signals, resulting in reduced bit rate and lower spectral efficiency. Compared to PI-DCSK, CCI-DCSK and MC-DCSK, 2CI-DCSK shows lower spectral efficiency as more subcarriers are occupied for index modulation. However, it can be observed in this table that the spectral efficiency of 2CI-DCSK is much higher (almost 2^{p+1} times) than those of CI-DCSK and CIM-DCSK systems. This is because that 2CI-DCSK system transmits two layers of data simultaneously over the same number of subcarriers.

TABLE 3. Spectral efficiency comparison.

Modulation	Spectral Efficiency
MC-DCSK	$(2p+2)/((2p+3)\cdot B\beta T_c)$
PI-DCSK	$(p+1)/B\beta T_c$
CCI-DCSK	$(2p+2)/B\beta T_c$
CIM-DCSK	$(2p+2)/((2^{2p+1}+1)\cdot B\beta T_c)$
CI-DCSK	$(2p+2)/((2^{2p+1}+1)\cdot B\beta T_c)$
2CI-DCSK	$(2p+2)/((2^{p}+1)\cdot B\beta T_c)$

C. COMPLEXITY ANALYSIS

For hardware complexity comparison, the elements that are needed to construct CIM-DCSK, 2CI-DCSK and CI-DCSK transmitters and receivers are listed in Table 4 and Table 5, respectively.

Compared to CIM-DCSK, 2CI-DCSK transmitter requires more multipliers, adders and extra Hilbert filter, but it avoids the usage of Walsh code generator, repeater, switcher, as well as the delay line. This makes 2CI-DCSK much easier to be implemented in UWB communications. At the receiver side, although 2CI-DCSK needs Hilbert filter and more matched filters, it not only avoids the usage of delay line, holder, Walsh code generator and switcher but also remarkably reduces the number of multipliers. Moreover, the hardware complexity increase caused by matched filters could be avoided if OFDM is employed to implement 2CI-DCSK transmission. In summary, the overall hardware complexity of 2CI-DCSK system is no higher than that of CIM-DCSK system.

TABLE 4. Transmitter hardware complexity comparison.

Elements	2CI-DCSK	CI-DCSK	CIM-DCSK
Adders	2^p+1	1	0
Multipliers	$3\cdot 2^p+1$	$2^{2p+2}+1$	2
Index mappers/ selectors	2	1	1
Polarity converters	2	1	1
Pulse shaping filters	2	1	0
Additional blocks	Hilbert filter	-	Delay line Repeater Switcher Walsh code generator

TABLE 5. Receiver hardware complexity comparison.

Elements	2CI-DCSK	CI-DCSK	CIM-DCSK
Multipliers	2^p+1	$2^{2p+1}+1$	2^{2p+1}
Matched filters	2^p+1	$2^{2p+1}+1$	0
Additional blocks	Hilbert filter	-	Delay line Holder Switcher Walsh code generator

Compared to CI-DCSK, 2CI-DCSK system requires additional circuits to implement two layers of code index modulations. That includes 2^p adders, one polarity converter, one index mapper, one pulse shaping filter in the transmitter (see Table 4), as well as two Hilbert filters on both sides (see Table 4 and 5). These modifications imply that 2CI-DCSK might need more complicated transceiver circuits in comparison to CI-DCSK. However, as 2CI-DCSK greatly reduces the numbers of multipliers and matched filters in transceivers, the aforementioned complexity increase in 2CI-DCSK could, to some extent, be compensated.

The analysis of computational complexity is based on the total number of multiplications performed for spreading/dispreading during one symbol duration. In 2CI-DCSK, 2^{p+1} spreading operations are performed by the transmitter to transmit one symbol that carries $2p+2$ bits, and 2^{p+1} correlations are performed by the receiver to recover such a symbol. Hence, the total number of multiplications required for 2CI-DCSK system in one symbol duration is

$$o_{2CI-DCSK} = 2^{p+1}\beta + 2^{p+1}\beta = 2^{p+2}\beta \tag{16}$$

Similarly, for CI-DCSK system it is

$$o_{CI-DCSK} = 2^{2p+1}\beta + 2^{2p+1}\beta = 2^{2p+2}\beta \tag{17}$$

According to [21], CIM-DCSK system requires $2+2\cdot 2^{2p+1}$ spreading/dispreading operations to transmit $2p+2$ bits. As chaotic reference length equals to β, $2^{2p+1}\beta$ multiplications are performed for each spreading/dispreading operation

in CIM-DCSK. As a result, the total number of multiplications performed by CIM-DCSK system in one symbol duration is

$$o_{CIM-DCSK} = (2 + 2 \cdot 2^{2p+1}) \cdot 2^{2p+1}\beta = (2^{2p+2} + 2^{4p+3})\beta \tag{18}$$

It can be found from (16), (17) and (18) that 2CI-DCSK system shows the lowest computational complexity among these three systems.

IV. BER PERFORMANCE ANALYSIS

In this section, the BER performance of the proposed system is analyzed over the multipath Rayleigh fading channel as well as the AWGN channel.

A. CHANNEL MODEL

Here, a multipath Rayleigh fading channel that consists of L independent and identically distributed Rayleigh slow fading paths is considered. This is a commonly used model for wireless communication systems [7], [9], [31], [32]. The output of such a channel is given by:

$$r(t) = \sum_{l=1}^{L} \alpha_l s(t - \tau_l T_c) + n(t) \tag{19}$$

where α_l and τ_l are the propagation gain and the chip delay of the l^{th} path, respectively, and $n(t)$ is an AWGN with power spectral density of $N_0/2$.

To facilitate the following analysis, the largest multipath delay is assumed to be much shorter than the symbol duration, i.e., $0 < \tau_{l\max} \ll \beta$, and thus the inter-symbol interference (ISI) is negligible compared to the interference within each symbol due to multipath time delay [31].

B. BER ANALYSIS

In 2CI-DCSK, two layers of carrier index modulations are performed on the same available subcarriers, resulting in possible collision in subcarrier activation. In our following analysis, two different cases will be considered:

Case 1: The same subcarrier is activated in two layers (collision);

Case 2: Different subcarriers are activated in two layers (no collision).

1) BER DERIVATION IN CASE 1

In this case, index bits in two data groups are identical, so the active subcarrier selected by the index selector in the first layer happens to be the one chosen by the index selector in the second layer. This implies that the total number of active subcarriers is 1. For the ease of analysis, we consider choosing the 1^{st} subcarrier as the active one during the v^{th} symbol period. Assuming that both the carrier and the chip are perfectly synchronized, the i^{th} elements of matrices $Z_v^{(1)}$ and $Z_v^{(2)}$ can be represented as:

$$Z_{v,i}^{(1)} = \begin{cases} \sum_{k=1}^{\beta}\left(\sum_{l=1}^{L}\alpha_{v,l}x_{v,k-\tau_l} + n_{v,k}^0\right) \\ \quad \times\left(\sum_{l=1}^{L}\alpha_{v,l}\left(d_{v,1}^{(1)}x_{v,k-\tau_l} + d_{v,1}^{(2)}y_{v,k-\tau_l}\right) + n_{v,k}^1\right), \\ \quad i = 1 \\ \sum_{k=1}^{\beta}\left(\sum_{l=1}^{L}\alpha_{v,l}x_{v,k-\tau_l} + n_{v,k}^0\right)n_{v,k}^i, \quad 1 < i \le 2^p \end{cases} \tag{20}$$

$$Z_{v,i}^{(2)} = \begin{cases} \sum_{k=1}^{\beta}\left(\sum_{l=1}^{L}\alpha_{v,l}y_{v,k-\tau_l} + \tilde{n}_{v,k}^0\right) \\ \quad \times\left(\sum_{l=1}^{L}\alpha_{v,l}\left(d_{v,1}^{(1)}x_{v,k-\tau_l} + d_{v,1}^{(2)}y_{v,k-\tau_l}\right) + n_{v,k}^1\right), \\ \quad i = 1 \\ \sum_{k=1}^{\beta}\left(\sum_{l=1}^{L}\alpha_{v,l}y_{v,k-\tau_l} + \tilde{n}_{v,k}^0\right)n_{v,k}^i, \quad 1 < i \le 2^p \end{cases} \tag{21}$$

with $n_{v,k}^i$ and $\tilde{n}_{v,k}^i$ representing the exact copy and Hilbert transform of the k^{th} sample of noise that affects the signal transmitted on the i^{th} subcarrier, respectively.

For large β, it can be easily obtained that:

$$\sum_{k=1}^{\beta} x_{v,k-l}x_{v,k-q} \approx 0, \quad l \ne q \tag{22}$$

Thus, the means and variances of $Z_{v,i}^{(1)}$ and $Z_{v,i}^{(1)}$ can be approximated as:

$$E\left[Z_{v,i}^{(1)}\right] \approx \begin{cases} \sum_{l=1}^{L}\alpha_{v,l}^2 E_c^v d_{v,1}^{(1)} = \mu, & i = 1 \\ 0, & 1 < i \le 2^p \end{cases} \tag{23}$$

$$E\left[Z_{v,i}^{(2)}\right] \approx \begin{cases} \sum_{l=1}^{L}\alpha_{v,l}^2 E_c^v d_{v,1}^{(2)}, & i = 1 \\ 0, & 1 < i \le 2^p \end{cases} \tag{24}$$

$$var\left[Z_{v,i}^{(1)}\right] = var\left[Z_{v,i}^{(2)}\right] \approx \begin{cases} 3\sum_{l=1}^{L}\alpha_{v,l}^2 E_c^v N_0 + N_0^2\beta = \sigma_1^2, & i = 1 \\ \sum_{l=1}^{L}\alpha_{v,l}^2 E_c^v N_0 + N_0^2\beta = \sigma_2^2, & 1 < i \le 2^p \end{cases} \tag{25}$$

where $E_c^v = \sum_{k=1}^{\beta} x_{v,k}^2$ and it is the energy of chaotic reference signal.

In each layer, unless the correlation magnitude for the active subcarrier is larger than the correlation magnitudes for all inactive subcarriers, an error will occur in the detection of index bits. Therefore, if the detection for index bits in the first layer is considered, the probability of correct detection for current index symbol can be obtained as:

$$P^{(1)}_{C\_index1} = Prob\left[\left|Z^{(1)}_{v,1}\right| > max\left(\left|Z^{(1)}_{v,i}\right|\right) | 1 < i \le 2^p\right] = \int_0^\infty \left(F_{\left|Z^{(1)}_{v,i}\right|}(r)\right)^{2^p-1} f_{\left|Z^{(1)}_{v,1}\right|}(r)\, dr \quad (26)$$

Here, $f_{\left|Z^{(1)}_{v,1}\right|}(r)$ is the probability density function (PDF) of $|Z^{(1)}_{v,1}|$, and $F_{\left|Z^{(1)}_{v,i}\right|}(r)$ is the cumulative distribution function (CDF) of $|Z^{(1)}_{v,i}|$ with $1 < i \le 2^p$. According to [33], $Z^{(1)}_{v,i}$ follows a Gaussian distribution with its mean and variance given in (23) and (25), respectively. As a result, $F_{\left|Z^{(1)}_{v,i}\right|}(r)$ and $f_{\left|Z^{(1)}_{v,1}\right|}(r)$ can be represented as:

$$F_{\left|Z^{(1)}_{v,i}\right|}(r) = erf\left(\frac{r}{\sqrt{2\sigma_2^2}}\right) \quad (27)$$

$$f_{\left|Z^{(1)}_{v,1}\right|}(r) = \frac{1}{\sqrt{2\pi\sigma_1^2}}\left(e^{-\frac{(r-\mu)^2}{2\sigma_1^2}} + e^{-\frac{(r+\mu)^2}{2\sigma_1^2}}\right) \quad (28)$$

where $erf(\cdot)$ denotes the error function [34]. Substituting (27) and (28) into (26), (26) can be simplified as:

$$P^{(1)}_{Cindex1} = \frac{1}{\sqrt{2\pi\sigma_1^2}} \int_0^\infty \left(erf\left(\frac{r}{\sqrt{2\sigma_2^2}}\right)\right)^{2^p-1} \times \left(e^{-\frac{(r-\mu)^2}{2\sigma_1^2}} + e^{-\frac{(r+\mu)^2}{2\sigma_1^2}}\right) dr \quad (29)$$

In a similar way, the probability of correct detection for current index symbol in the second layer can also be derived, which turns out to be identical to (29). Thus the symbol error probability for the index symbols can be written as:

$$P_{SER\_index1} = 1 - \frac{1}{\sqrt{2\pi\sigma_1^2}} \int_0^\infty \left(erf\left(\frac{r}{\sqrt{2\sigma_2^2}}\right)\right)^{2^p-1} \times \left(e^{-\frac{(r-\mu)^2}{2\sigma_1^2}} + e^{-\frac{(r+\mu)^2}{2\sigma_1^2}}\right) dr \quad (30)$$

Based on the relationship between bit error probability and symbol error probability, the bit error probability of index bits can be derived as:

$$P_{\mathrm{BER}_index1} = \sum_{e=1}^{p} \frac{C(p,e)}{2^p - 1} \frac{e}{p} P_{\mathrm{SER}_index1} \quad (31)$$

where $C(p,e) = \frac{p!}{e!(p-e)!}$.

If a wrong decision is made in the detection of index bits, an inactive subcarrier will be mistaken for the active one, leading to equal probabilities (i.e., 1/2) of correct and false decisions in modulated bit detection in each layer. With a correct decision in index bits detection, the error detection probability for the modulated bit in the first layer can be calculated by:

$$prob\left(sign\left(Z^{(1)}_{v,1}\right) \ne d^{(1)}_{v,1}\right) = \frac{1}{2} erfc\left(\frac{|\mu|}{\sqrt{2\sigma_1^2}}\right) \quad (32)$$

Similarly, we can prove that the error detection probability for the modulated bit in the second layer can also be evaluated by (32). Therefore, the bit error probability of modulated bits is represented as:

$$P_{\mathrm{BER\_mod\ 1}} = \frac{1}{2} erfc\left(\frac{|\mu|}{\sqrt{2\sigma_1^2}}\right)\left(1 - P_{SER\_index1}\right) + \frac{1}{2} P_{SER\_index1} \quad (33)$$

Same conclusions as (31) and (33) can be derived when other subcarrier (rather than the 1st one) is activated. Considering that data bits in each group are divided into two types, i.e., p index bits and 1 modulated bit, the BER of the system in Case 1 is a linear combination of (31) and (33). It can be derived as:

$$P_{BER1} = \frac{p}{p+1} P_{BER\_index1} + \frac{1}{p+1} P_{BER\_mod1} \quad (34)$$

2) BER DERIVATION IN CASE 2

In this case, index bits in two data groups are different. As a result, two different subcarriers are activated in two layers, and the chaotic signal and its Hilbert transform are modulated onto different subcarriers. In the v^{th} symbol duration, it is assumed that the j^{th} and the m^{th} subcarriers ($m \ne j$) are activated by the first and second layers, respectively. In consequence, the i^{th} elements of matrices $\boldsymbol{Z}^{(1)}_v$ and $\boldsymbol{Z}^{(2)}_v$ can be rewritten as:

$$Z^{(1)}_{v,i} = \begin{cases} \sum_{k=1}^{\beta}\left(\sum_{l=1}^{L} \alpha_{v,l} x_{v,k-\tau_l} + n^0_{v,k}\right)\left(\sum_{l=1}^{L} \alpha_{v,l} d^{(1)}_{v,j} x_{v,k-\tau_l} + n^j_{v,k}\right), \\ \qquad i = j \\ \sum_{k=1}^{\beta}\left(\sum_{l=1}^{L} \alpha_{v,l} x_{v,k-\tau_l} + n^0_{v,k}\right)\left(\sum_{l=1}^{L} \alpha_{v,l} d^{(2)}_{v,m} y_{v,k-\tau_l} + n^m_{v,k}\right), \\ \qquad i = m \\ \sum_{k=1}^{\beta}\left(\sum_{l=1}^{L} \alpha_{v,l} x_{v,k-\tau_l} + n^0_{v,k}\right) n^i_{v,k}, \\ \qquad 1 \le i \le 2^p, \quad i \ne j \ne m \end{cases} \quad (35)$$

$$Z_{v,i}^{(2)} = \begin{cases} \sum_{k=1}^{\beta}\left(\sum_{l=1}^{L}\alpha_{v,l}y_{v,k-\tau_l}+\tilde{n}_{v,k}^{0}\right)\left(\sum_{l=1}^{L}\alpha_{v,l}d_{v,j}^{(1)}x_{v,k-\tau_l}+n_{v,k}^{j}\right), \\ \qquad i=j \\ \sum_{k=1}^{\beta}\left(\sum_{l=1}^{L}\alpha_{v,l}y_{v,k-\tau_l}+\tilde{n}_{v,k}^{0}\right)\left(\sum_{l=1}^{L}\alpha_{v,l}d_{v,m}^{(2)}y_{v,k-\tau_l}+n_{v,k}^{m}\right), \\ \qquad i=m \\ \sum_{k=1}^{\beta}\left(\sum_{l=1}^{L}\alpha_{v,l}y_{v,k-\tau_l}+\tilde{n}_{v,k}^{0}\right)n_{v,k}^{i}, \\ \qquad 1\le i\le 2^p, \quad i\ne j\ne m \end{cases} \tag{36}$$

Based on (22), the means and variances of $Z_{v,i}^{(1)}$ and $Z_{v,i}^{(2)}$ can be approximated as:

$$E\left[Z_{v,i}^{(1)}\right] \approx \begin{cases} \sum_{l=1}^{L}\alpha_{v,l}^2E_c^v d_{v,j}^{(1)} = \mu, \quad i=j \\ 0, \quad 1\le i\le 2^p,\ i\ne j \end{cases} \tag{37}$$

$$E\left[Z_{v,i}^{(2)}\right] \approx \begin{cases} \sum_{l=1}^{L}\alpha_{v,l}^2E_c^v d_{v,m}^{(2)}, \quad i=m \\ 0, \quad 1\le i\le 2^p,\ i\ne m \end{cases} \tag{38}$$

$$var\left[Z_{v,i}^{(1)}\right] = var\left[Z_{v,i}^{(2)}\right] \approx \begin{cases} 2\sum_{l=1}^{L}\alpha_{v,l}^2E_c^vN_0+N_0^2\beta=\sigma_3^2, \\ \qquad i=j\ or\ i=m \\ \sum_{l=1}^{L}\alpha_{v,l}^2E_c^vN_0+N_0^2\beta=\sigma_2^2, \\ \qquad 1\le i\le 2^P, \quad i\ne j\ne m \end{cases} \tag{39}$$

Let us consider the detection for index bits in the first layer, the probability of correct detection for current index symbol can be obtained as:

$$\begin{aligned} P_{C_index2}^{(1)} &= Prob\left[\left|Z_{v,j}^{(1)}\right| > max\left(\left|Z_{v,i}^{(1)}\right|\right) | i\ne j\right] \\ &= \int_0^{\infty}\left(F_{\left|Z_{v,i}^{(1)}\right|}(r)\right)^{2^p-1} f_{\left|Z_{v,j}^{(1)}\right|}(r)\,dr \end{aligned} \tag{40}$$

where $F_{\left|Z_{v,i}^{(1)}\right|}(r)$ and $f_{\left|Z_{v,j}^{(1)}\right|}(r)$ can be represented as:

$$F_{\left|Z_{v,i}^{(1)}\right|}(r) = \begin{cases} erf\left(\frac{r}{\sqrt{2\sigma_3^2}}\right), & i=m \\ erf\left(\frac{r}{\sqrt{2\sigma_2^2}}\right), & i\ne m \end{cases} \tag{41}$$

$$f_{\left|Z_{v,j}^{(1)}\right|}(r) = \frac{1}{\sqrt{2\pi\sigma_3^2}}\left(e^{-\frac{(r-\mu)^2}{2\sigma_3^2}}+e^{-\frac{(r+\mu)^2}{2\sigma_3^2}}\right) \tag{42}$$

Substituting (41) and (42) into (40), (40) can be simplified as:

$$P_{C\_index2}^{(1)} = \frac{1}{\sqrt{2\pi\sigma_3^2}}\int_0^{\infty}\left(erf\left(\frac{r}{\sqrt{2\sigma_2^2}}\right)\right)^{2^p-2} erf\left(\frac{r}{\sqrt{2\sigma_3^2}}\right) \times\left(e^{-\frac{(r-\mu)^2}{2\sigma_3^2}}+e^{-\frac{(r+\mu)^2}{2\sigma_3^2}}\right)dr \tag{43}$$

As the derived probability of correct detection for current index symbol in the second layer can also be evaluated by (43), the symbol error probability for the index symbols can be written as:

$$P_{SER\_index2} = 1-\frac{1}{\sqrt{2\pi\sigma_3^2}}\int_0^{\infty}\left(erf\left(\frac{r}{\sqrt{2\sigma_2^2}}\right)\right)^{2^p-2} \times erf\left(\frac{r}{\sqrt{2\sigma_3^2}}\right)\left(e^{-\frac{(r-\mu)^2}{2\sigma_3^2}}+e^{-\frac{(r+\mu)^2}{2\sigma_3^2}}\right)dr \tag{44}$$

The bit error probability of index bits can be denoted as:

$$P_{\mathrm{BER}\_index2} = \sum_{e=1}^{p}\frac{C(p,e)}{2^p-1}\frac{e}{p}P_{\mathrm{SER}\_index2} \tag{45}$$

If the detection for index bits is correct, $Z_{v,j}^{(1)}$ and $Z_{v,m}^{(2)}$ will be compared to threshold zero to recover the modulated bits in the first and second layers, respectively. Consequently, the error detection probability for the modulated bit in the first layer can be calculated by:

$$prob\left(sign\left(Z_{v,j}^{(1)}\right)\ne d_{v,j}^{(1)}\right) = \frac{1}{2}erfc\left(\frac{|\mu|}{\sqrt{2\sigma_3^2}}\right) \tag{46}$$

In a similar way, the error detection probability for the modulated bit in the second layer can also be proved to be equal to (46). Thus the bit error probability of modulated bits is represented as:

$$P_{\mathrm{BER}\_\mathrm{mod}\,2} = \frac{1}{2}erfc\left(\frac{|\mu|}{\sqrt{2\sigma_3^2}}\right)\left(1-P_{SER\_index2}\right) + \frac{1}{2}P_{SER\_index2} \tag{47}$$

As a linear combination of (45) and (47), the BER of the system in Case 2 can be derived as:

$$P_{BER2} = \frac{p}{p+1}P_{BER\_index2}+\frac{1}{p+1}P_{BER\_mod2} \tag{48}$$

3) OVERALL BER FORMULA

Under the assumption that the transmitted data bits are equiprobable, the overall bit error rate of 2CI-DCSK system can be obtained as:

$$P_{BER} = \frac{1}{2^p}P_{BER1}+\frac{2^p-1}{2^p}P_{BER2} \tag{49}$$

Defining $\gamma_b = \frac{3\sum_{l=1}^{L}\alpha_{v,l}^2 E_c^v}{4(p+1)N_0}$ and $\bar{\gamma}_c = \frac{3E\left[\alpha_{v,l}^2\right]E_c^v}{4(p+1)N_0}$, the overall BER formula of the proposed system over the multipath Rayleigh fading channel can be obtained by averaging the BER in (49) over γ_b:

$$P_{Rayleigh} = \int_0^{+\infty} P_{BER} f(\gamma_b)\, d\gamma_b \tag{50}$$

In which,

$$f(\gamma_b) = \frac{\gamma_b^{L-1}}{(L-1)!\bar{\gamma}_c^L} e^{-\left(\frac{\gamma_b}{\bar{\gamma}_c}\right)} \tag{51}$$

This expression is also applicable to the AWGN situation, for which only the first path with propagation gain $\alpha_1 = 1$ and chip delay $\tau_1 = 0$ is considered.

V. SIMULATION RESULTS AND DISCUSSIONS

In order to validate former analysis, BER performances of 2CI-DCSK, CI-DCSK, CIM-DCSK, PI-DCSK, CCI-DCSK, MC-DCSK and DCSK systems are simulated and compared under different channel conditions. In our simulation, an AWGN channel, a two-path Rayleigh fading channel and a three-path Rayleigh fading channel are considered. The statistical parameters of the two-path and three-path Rayleigh fading channel models are $E[\alpha_1^2] = E[\alpha_2^2] = 1/2$ and $E[\alpha_1^2] = E[\alpha_2^2] = E[\alpha_3^2] = 1/3$, respectively. The chip delays for the two-path and three-path models are $\tau_1 = 0$, $\tau_2 = 2$ and $\tau_1 = 0$, $\tau_2 = 1$, $\tau_3 = 2$, respectively.

A. BER PERFORMANCE VERIFICATION

In Fig.2, the simulated performances of the proposed system are compared to the analytical ones calculated by (50) over AWGN and multipath Rayleigh fading channels, respectively. It is obvious that the simulated results and analytical BER predictions match quite well in all channels, confirming the correctness of our analysis in Section IV.

The impacts of β on the BER performance of 2CI-DCSK are studied over different channels in Fig.3 and Fig.4. It is noted in Fig.3 that there is an obvious gap between analytical and simulated results when β is small. As β increases, the gap gradually disappears. This disagreement is due to the limitation of Gaussian approximation. Besides, in Fig.3, it is also observed that there is an optimal value of β that would help the proposed system to perform best. Similar phenomena have also been observed in many other chaos-based communication systems [8], [9]. As shown in Fig.3 and Fig.4, BER performances of 2CI-DCSK degrade with β. This can be explained by the fact that more and more noise components will be involved when β increases.

Since ISI ignored in BER derivation grows with chip delay, derived BER formula in section IV might be inaccurate for multipath Rayleigh fading channels with large chip delays. For this reason, the effect of chip delay on the BER performance of 2CI-DCSK is evaluated in Fig.5. In this figure, although the simulated performance deteriorates with chip delay τ_2, the computed results agree with the simulated ones for $\tau_2 < 10$.

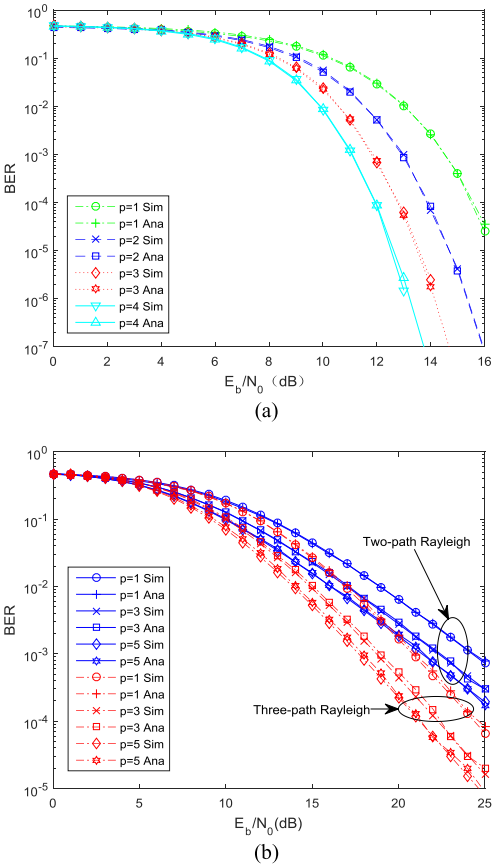

FIGURE 2. Simulated and analytical BER performances of 2CI-DCSK with β=128 for various p. (a) AWGN channel. (b) Multipath Rayleigh fading channels.

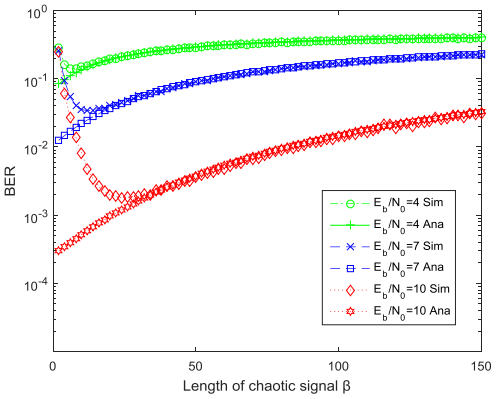

FIGURE 3. BER performances of 2CI-DCSK versus β over an AWGN channel for p=3.

B. PERFORMANCE COMPARISON WITH OTHER SCHEMES

In Fig.6, the BER performances of 2CI-DCSK, CI-DCSK, MC-DCSK and DCSK systems are compared over the AWGN and three-path Rayleigh fading channels. Here, the chaotic sequence length β is set to 128 for all systems.

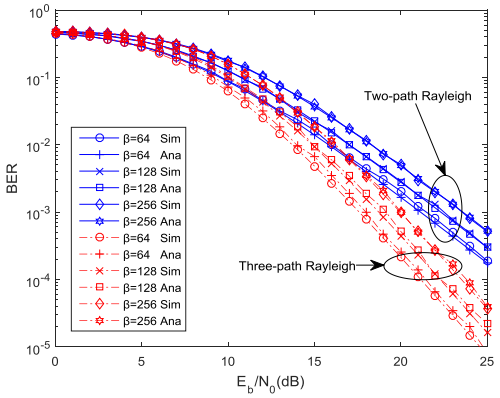

FIGURE 4. BER performance of 2CI-DCSK over multipath Rayleigh fading channels with p=3.

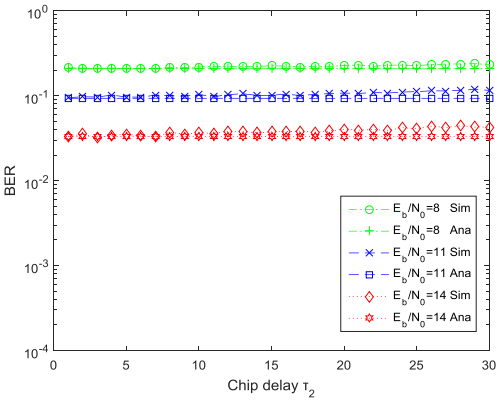

FIGURE 5. BER performances of 2CI-DCSK with β=128 and p=3 for various signal noise ratios over a two-path Rayleigh fading channel.

In Fig.6 (a), the number of subcarriers is set to 65 for all multi-carrier systems, including 2CI-DCSK, CI-DCSK and MC-DCSK. It is obvious in this figure that the proposed system outperforms the other systems in both AWGN and multipath Rayleigh fading channels. Besides, compared to CI-DCSK with the same number of subcarriers, 2CI-DCSK not only further improves the BER performance but also doubles the bit rate as two layers of index modulations are adopted.

In Fig.6 (b), all systems except DCSK transmit 10 bits in one symbol. As shown in this figure, 2CI-DCSK and CI-DCSK systems perform much better than MC-DCSK and DCSK in both channels. This performance improvement is attributed to the carrier index modulation. It is also noted that the BER performance of CI-DCSK is superior to that of 2CI-DCSK in AWGN channel, but this superiority becomes invisible in multipath Rayleigh fading channel. In fact, CI-DCSK system pays a high price for the BER superiority over 2CI-DCSK with the same number of bits per symbol. To transmit 10 bits in one symbol, CI-DCSK requires 513 subcarriers, but only 17 subcarriers are needed in 2CI-DCSK. This means that CI-DCSK sacrifices a lot of subcarrier resources and increases system complexity (see section III.C) for BER performance improvement.

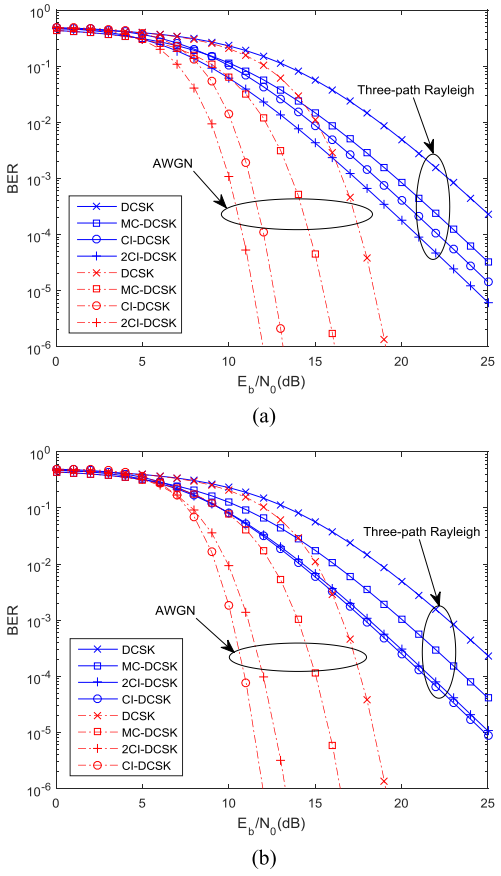

FIGURE 6. Performance comparison between DCSK, MC-DCSK, CI-DCSK and 2CI-DCSK systems over the AWGN and three-path Rayleigh fading channels. (a) Fixed number of subcarriers. (b) Fixed number of bits per symbol.

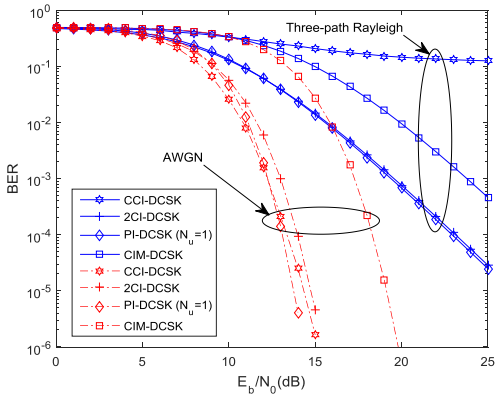

FIGURE 7. Performance comparison between 2CI-DCSK, PI-DCSK, CCI-DCSK and CIM-DCSK systems with same transmitted bits per symbol over AWGN and three-path Rayleigh fading channels.

Fig.7 plots and compares the BER performances of 2CI-DCSK, PI-DCSK, CCI-DCSK and CIM-DCSK systems in different channels. In these systems, the chaotic sequence length β is set to 128, and the number of transmitted bits per symbol is 6. It is observed in this figure that 2CI-DCSK outperforms CIM-DCSK in both channels. Compared to PI-DCSK and CCI-DCSK, 2CI-DCSK performs slightly

worse in AWGN channel. In multipath Rayleigh fading channel, BER performances of 2CI-DCSK and PI-DCSK systems are almost the same, while the performance of CCI-DCSK system deteriorates seriously due to non-negligible ISI. In fact, the performance improvements in PI-DCSK and CCI-DCSK systems in AWGN channel can only be supported by the decrease of energy efficiency (see Section III.A) and the increase of decoding complexity. For instance, if 10 bits are sent in one symbol, CCI-DCSK and PI-DCSK detectors have to perform 512 correlations so that all possible permutation/ commutation combinations could be searched. However, 2CI-DCSK detector only needs to perform 32 correlations, as two layers of index modulations share the same 16 subcarrier activation combinations. Therefore, 2CI-DCSK system is more suitable for many low cost, high data rate and low complexity wireless communication scenarios.

VI. CONCLUSION

In this paper, a novel efficient carrier index differential chaos shift keying modulation system has been designed and analyzed. For high-data-rate transmission, two layers of carrier index modulations are performed in the proposed system. Both layers share not only the same available subcarriers but also the same chaotic reference signal, leading to increased energy efficiency and spectral efficiency in comparison with CI-DCSK. With the help of Hilbert transform, data-bearing signals at different layers are kept to be orthogonal, resulting in minimized interferences between two layers. The BER performances of the proposed 2CI-DCSK system over AWGN and multipath Rayleigh fading channels are analyzed and verified by Monte Carlo simulations. Compared to CI-DCSK, 2CI-DCSK system achieves higher bit rate, increased energy and spectral efficiencies, and even better BER performance. Besides, compared to MC-DCSK, 2CI-DCSK shows noticeable superiority in energy efficiency and BER performance at the cost of affordable decreases in spectral efficiency.

REFERENCES

[1] A. Abel and W. Schwarz, "Chaos communications-principles, schemes, and system analysis," *Proc. IEEE*, vol. 90, no. 5, pp. 691–710, May 2002.

[2] S. Wang and X. Wang, "*M*-DCSK-based chaotic communications in MIMO multipath channels with no channel state information," *IEEE Trans. Circuits Syst. II, Exp. Briefs*, vol. 57, no. 12, pp. 1001–1005, Dec. 2010.

[3] Y. Fang, G. Han, P. Chen, F. C. M. Lau, G. Chen, and L. Wang, "A survey on DCSK-based communication systems and their application to UWB scenarios," *IEEE Commun. Surveys Tuts.*, vol. 18, no. 3, pp. 1804–1837, 3rd Quart., 2016.

[4] H. Yang and G.-P. Jiang, "High-efficiency differential-chaos-shift-keying scheme for chaos-based noncoherent communication," *IEEE Trans. Circuits Syst. II, Exp. Briefs*, vol. 59, no. 5, pp. 312–316, May 2012.

[5] G. Kaddoum, E. Soujeri, and Y. Nijsure, "Design of a short reference noncoherent chaos-based communication systems," *IEEE Trans. Commun.*, vol. 64, no. 2, pp. 680–689, Jan. 2016.

[6] W. Xu and L. Wang, "Performance optimization for short reference differential chaos shift keying scheme," in *Proc. IEEE Int. Conf. Signal Process., Commun. Comput. (ICSPCC)*, Xiamen, China, Oct. 2017, pp. 1–6.

[7] W. K. Xu, L. Wang, and G. Kolumbán, "A novel differential chaos shift keying modulation scheme," *Int. J. Bifurcation Chaos*, vol. 21, pp. 799–814, Mar. 2011.

[8] W. K. Xu, L. Wang, and G. Kolumbán, "A new data rate adaption communications scheme for code-shifted differential chaos shift keying modulation," *Int. J. Bifurcation Chaos*, vol. 22, no. 8, pp. 1250201-1–1250201-8, Aug. 2012.

[9] G. Kaddoum, F. Richardson, and F. Gagnon, "Design and analysis of a multi-carrier differential chaos shift keying communication system," *IEEE Trans. Commun.*, vol. 61, no. 8, pp. 3281–3291, Aug. 2013.

[10] Z. Galias and G. M. Maggio, "Quadrature chaos-shift keying: Theory and performance analysis," *IEEE Trans. Circuits Syst. I, Fundam. Theory Appl.*, vol. 48, no. 12, pp. 1510–1519, Dec. 2001.

[11] L. Wang, G. Cai, and G. R. Chen, "Design and performance analysis of a new multiresolution *M*-ary differential chaos shift keying communication system," *IEEE Trans. Wireless Commun.*, vol. 14, no. 9, pp. 5197–5208, Sep. 2015.

[12] G. Cai, Y. Fang, G. Han, F. C. M. Lau, and L. Wang, "A square-constellation-based *M*-ary DCSK communication system," *IEEE Access*, vol. 4, pp. 6295–6303, Nov. 2016.

[13] G. Cai, Y. Fang, and G. Han, "Design of an adaptive multiresolution *M*-ary DCSK system," *IEEE Commun. Lett.*, vol. 21, no. 1, pp. 60–63, Jan. 2017.

[14] G. Cai, Y. Fang, G. Han, L. Wang, and G. Chen, "A new hierarchical *M*-ary DCSK communication system: Design and analysis," *IEEE Access*, vol. 5, pp. 17414–17424, Oct. 2017.

[15] Y. Fang, L. Wang, X. Jing, P. Chen, G. Chen, and W. Xu, "Design and analysis of a DCSK-ARQ/CARQ system over multipath fading channels," *IEEE Trans. Circuits Syst. I, Reg. Papers*, vol. 62, no. 6, pp. 1637–1647, Jun. 2015.

[16] Y. Fang, L. Xu, L. Wang, and G. Chen, "Performance of MIMO relay DCSK-CD systems over Nakagami fading channels," *IEEE Trans. Circuits Syst. I, Reg. Papers*, vol. 60, no. 3, pp. 757–767, Mar. 2013.

[17] E. Basar, M. Wen, R. Mesleh, M. Di Renzo, Y. Xiao, and H. Haas, "Index modulation techniques for next-generation wireless networks," *IEEE Access*, vol. 5, pp. 16693–16746, 2017.

[18] G. Kaddoum, M. F. A. Ahmed, and Y. Nijsure, "Code index modulation: A high data rate and energy efficient communication system," *IEEE Commun. Lett.*, vol. 19, no. 2, pp. 175–178, Feb. 2015.

[19] G. Kaddoum, Y. Nijsure, and T. Hung, "Generalized code index modulation technique for high-data-rate communication systems," *IEEE Trans. Veh. Technol.*, vol. 65, no. 9, pp. 7000–7009, Sep. 2016.

[20] W. Xu, T. Huang, and L. Wang, "Code-shifted differential chaos shift keying with code index modulation for high data rate transmission," *IEEE Trans. Commun.*, vol. 65, no. 10, pp. 4285–4294, Oct. 2017.

[21] W. Xu, Y. Tan, F. C. M. Lau, and G. Kolumbán, "Design and optimization of differential chaos shift keying scheme with code index modulation," *IEEE Trans. Commun.*, vol. 66, no. 5, pp. 1970–1980, May 2018.

[22] T. Huang, L. Wang, W. Xu, and F. C. M. Lau, "Multilevel code-shifted differential-chaos-shift-keying system," *IET Commun.*, vol. 10, no. 10, pp. 1189–1195, Jul. 2016.

[23] Y. Tan, W. Xu, T. Huang, and L. Wang, "A multilevel code shifted differential chaos shift keying scheme with code index modulation," *IEEE Trans. Circuits Syst. II, Exp. Briefs*, to be published, doi: 10.1109/TCSII.2017.2764916.

[24] E. Soujeri, G. Kaddoum, and M. Herceg, "Design of an initial condition-index chaos shift keying modulation," *Electron. Lett.*, vol. 54, no. 7, pp. 447–449, Apr. 2018.

[25] H. Yang, W. K. S. Tang, G. Chen, and G.-P. Jiang, "System design and performance analysis of orthogonal multi-level differential chaos shift keying modulation scheme," *IEEE Trans. Circuits Syst. I, Reg. Papers*, vol. 63, no. 1, pp. 146–156, Jan. 2016.

[26] M. Herceg, G. Kaddoum, D. Vranješ, and E. Soujeri, "Permutation index DCSK modulation technique for secure multiuser high-data-rate communication systems," *IEEE Trans. Veh. Technol.*, vol. 67, no. 4, pp. 2997–3011, Apr. 2018.

[27] M. Herceg, D. Vranješ, G. Kaddoum, and E. Soujeri, "Commutation code index DCSK modulation technique for high-data-rate communication systems," *IEEE Trans. Circuits Syst. II, Exp. Briefs*, to be published, doi: 10.1109/TCSII.2018.2817930.

[28] E. Başar, Ü. Aygölü, E. Panayirci, and H. V. Poor, "Orthogonal frequency division multiplexing with index modulation," *IEEE Trans. Signal Process.*, vol. 61, no. 22, pp. 5536–5549, Nov. 2013.

[29] E. Soujeri, G. Kaddoum, M. Au, and M. Herceg, "Frequency index modulation for low complexity low energy communication networks," *IEEE Access*, vol. 5, pp. 23276–23287, Jun. 2017.

[30] M. Au, G. Kaddoum, F. Gagnon, and E. Soujeri. (2017). "A joint code-frequency index modulation for low-complexity, high spectral and energy efficiency communications." [Online]. Available: https://arxiv.org/abs/1712.07951
[31] G. Cheng, L. Wang, W. Xu, and G. Chen, "Carrier index differential chaos shift keying modulation," *IEEE Trans. Circuits Syst. II, Exp. Briefs*, vol. 64, no. 8, pp. 907–911, Aug. 2017.
[32] H. Yang, W. K. S. Tang, G. Chen, and G.-P. Jiang, "Multi-carrier chaos shift keying: System design and performance analysis," *IEEE Trans. Circuits Syst. I, Reg. Papers*, vol. 64, no. 8, pp. 2182–2194, Aug. 2017.
[33] N. I. Chernov, "Limit theorems and Markov approximations for chaotic dynamical systems," *Probab. Theory Rel. Fields*, vol. 101, no. 3, pp. 321–362, Sep. 1995.
[34] B. Sklar, *Digital Communications: Fundamentals and Applications*. Englewood Cliffs, NJ, USA: Prentice-Hall, 1988.

WENHAO DAI received the B.E. degree from Jiaxing University, Jiaxing, China, in 2016. He is currently pursuing the M.E. degree in circuits and systems with the Nanjing University of Posts and Telecommunications, Nanjing, China. His research interests include chaos-based communications and deep learning.

HUA YANG (M'16) received the B.E. degree in automation and the Ph.D. degree in information and communication engineering from the Nanjing University of Posts and Telecommunications, China, in 2003 and 2014, respectively. Since 2014, she has been an Assistant Professor with the School of Electronic and Optical Engineering, Nanjing University of Posts and Telecommunications. In 2016, she was a Post-Doctoral Fellow with the Department of Electronic Engineering, City University of Hong Kong. Her current research interests include nonlinear circuits and systems and chaos-based communications.

YURONG SONG received the Ph.D. degree in information and telecommunication engineering from the Nanjing University of Posts and Telecommunications, Nanjing, China, in 2010. In 2012, she visited the Department of Electronic Engineering, City University of Hong Kong. She is currently a Professor with the Nanjing University of Posts and Telecommunications. Her main research interests lie in nonlinear dynamics, spreading dynamic of complex networks, and social networks.

GUOPING JIANG (M'03–SM'16) received the Ph.D. degree in control theory and engineering from Southeast University, Nanjing, China, in 1997. He is currently a Professor and the Vice President with the Nanjing University of Posts and Telecommunications, Nanjing, China. He has authored or coauthored over 200 published articles and two books in the area of nonlinear systems and control. His current research interests include chaos synchronization and control, chaos-based communication, and complex dynamical networks. He received the Awards for the New Century Excellent Talents of the Ministry of Education, China, in 2006, and the Awards for the 333 Project High-level Talents of Jiangsu Province, China, in 2011.